Journal of ELECTRICAL ENGINEERING, VOL. 58, NO. 2, 2007, 85–90

A ROTOR CONSISTING OF TWO IRON CYLINDERS FOR SWITCHED RELUCTANCE MOTORS

Eyhab El-kharashi *

The shaft in a conventional switched reluctance motor with multi-rotor teeth fills up a relatively high interior volume. However, it does not contribute in producing any torque. It is there only for mechanical purposes. Additionally, the conventional toothed rotor produces high torque ripples. These two points force to come up with a new design for the switched reluctance motor rotor that can rotate inside the stator without a shaft while grading the reluctance of the air gap to produce an output torque with low ripples. This paper introduces a new rotor design that consists of two solid iron cylinders. In the proposed design, there is no need for the shaft. The use of two cylinders grades the air gap, consequently producing a torque with low ripples.

K e y w o r d s: finite element methods, flux linkage characteristic, rotor design, switched reluctance motors, torque characteristic

1 INTRODUCTION

The switched reluctance motor (SRM) is the simplest motor among all the rotating machinery and it is the more efficient. The simplicity is due to the absence of any kind of windings, permanent magnets, or brushes on the rotor, whereas the efficiency is due to the absence of the copper loss in the rotor. These reasons plus the recent advent of the semiconductors encourage motor designers to focus on the design of SRMs to modify the classical methods of design to overcome the problems in conventional designs. This would enable SRMs to compete competitively with the rest of the electric motors to be the work horse of the industry [1].

Figure 1 shows the rotor of a conventional SRM. The shaft fills a relatively big interior volume without producing any torque. The rotor in this shape serves only mechanical purposes. Also the rotor in this toothed shape produces high torque ripples. So, it is necessary to design a new rotor that can rotate inside an SRM without having a shaft and produces output a torque with low ripples [2-3].

Figure 2 shows the proposed design of an SRM rotor. In this design, the rotor consists of two cylinders, changing entirely the topology of the rotor. There is no need for shaft and the air gap is graded, which smoothes the reluctance variation and consequently reduces the output torque ripples. The stator has wide six teeth to increase and concentrate the flux crossing from the stator to the rotor and six thin teeth as return flux teeth.

The SRM is inherently non-linear. Because of the double saliency, the air gap is non-uniform. Thus, the motor is designed to operate in saturated region of flux. The distribution of the electromagnetic field in an SRM is determined by solving Maxwell's field equations with given boundary conditions. Since the closed form solutions to Maxwell equations are very difficult or impossible to obtain for such a machine having complicated geometries and nonlinear materials, the numerical solution of the Maxwell equations becomes a necessity. The method of finite elements (FE) is an excellent numerical method for structures with complicated geometries and material nonlinearities. So, the characteristic of the proposed SRM rotor design is obtained here by the adaptive finite elements [4–7].

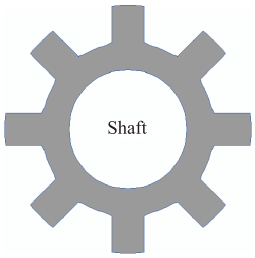

Fig. 1. Rotor of a conventional SRM.

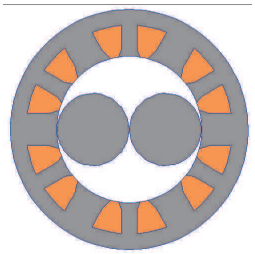

Fig. 2. Cross section of the proposed SRM rotor.

This paper is organized as follows. Section 2 describes in details the operation of the proposed SRM. Section 3 shows how to model the proposed design using finite elements.

2 OPERATION OF THE PROPOSED SRM

The proposed SRM has three phases in the stator. Each phase fills four slots: two on one side of the stator diameter and the others on the other side of the diameter. When one phase is energized there are different positions for the rotor cylinders. If the two cylinders are on the same line of the excited teeth, as shown in Fig. 3, the inductance is at its maximum. This position is defined as the aligned position.

* Faculty of Engineering, Electrical Power and Machines Department, Ain Shams University, 1 El-Sarayat Street, Abdou Basha Square, Abbassia, 11517 Cairo, Egypt; E-mail: EyhabElkharahi@hotmail.com

ISSN 1335-3632

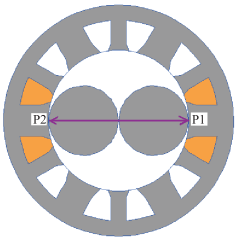

Fig. 3. SRM aligned position.

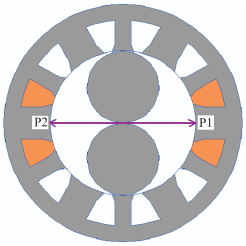

Fig. 4. SRM unaligned position.

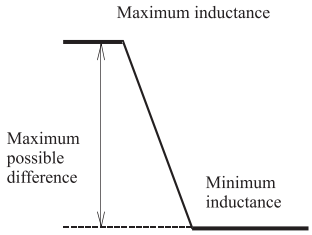

Fig. 5. Maximizing the gap between the extremal inductances.

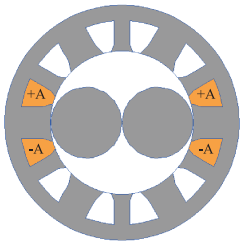

Fig. 6. One phase energized of the proposed two-cylindrical rotor SRM.

When the air gap between the two energized wide teeth is at its maximum, as shown in Fig. 4, the reluctance is at its maximum. This position is defined as the unaligned position.

The inductance in the aligned position is at its maximum value because the magnetic material fills the line between the two energized stator poles. On the other hand, the inductance in the unaligned position is at its minimum value because no magnetic material fills the line between the two energized stator poles. As the gap between the maximum and the minimum inductance positions is maximized; it is expected that this arrangement give the maximum possible torque from this volume (Fig. 5).

The reluctance torque is developed by energizing a pair of stator wide teeth on the same diameter. When the rotor poles are in a position of misalignment with the energized stator poles, they rotate to align themselves with the energized poles to be in the maximum inductance position (the only stable position). Continuous rotation is developed by energizing and deenergising the stator wide teeth [8].

The air gap length between the rotor outside diameter and bore diameter of the stator of the proposed SRM is made very small (0.3 mm) so that the motor can be operated under saturated conditions. This leads to high co-energy change as the rotor moves from the maximum to the minimum reluctance positions compared with that in unsaturated conditions. Hence, the motor develops the highest torque. The outside stator diameter of the new SRM design is 150 mm, the stator bore diameter is 91.4 mm, and the axial stator length is 150 mm.

3 MODELING THE PROPOSED SRM BY FINITE ELEMENTS

The proposed new SRM is a 3-phase symmetrical machine. The modeling shown here is for only one phase. Figure 6 shows the windings of one phase when it is in the aligned position. The flow chart in Fig. 7 shows the finite element solution steps. Figure 8 shows the first step in the solution. The aim of this step is to generate a set of objects to define the geometry of the two-cylinder rotor. These objects are defined by co-ordinate pairs that are taken in counter clockwise order, defining successive vertices of a polygonal figure defining the component. In the proposed SRM design, there are five objects: the stator, the air gap, the two coils, and the rotor (two solid iron cylinders) [9]. This way of representing the machine means that curved surfaces are represented as a series of straight lines. Therefore, an adequate number of points need to be used, particularly in the important air gap area. The object definition is used to create an initial mesh.

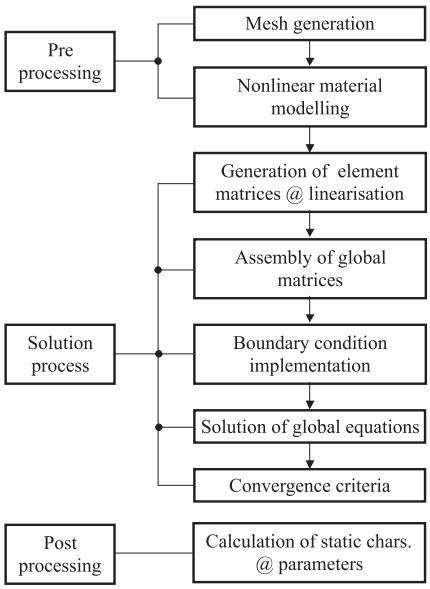

Fig. 7. A flow chart showing the solution steps using finite elements.

The geometry and layout of the machine is known from the design synthesis stage and, consequently, the information required to define iron saturation curves ($B(H)$), conductor positions, and boundary conditions are all on hand. The task is merely to map this information onto the initial finite element mesh. Figure 9 shows the boundary conditions of the proposed new design. The location of the phase conductor is shown and number *2 means this surface has the same potential.

The initial mesh is very coarse, thus the use of this mesh will produce gross error. The automatic method used here is based on the ability to estimate the error present in trial solutions. Given this ability, it is then possible to add nodes, where the error is the highest. As nodes are added, it is necessary to reform the elemen-

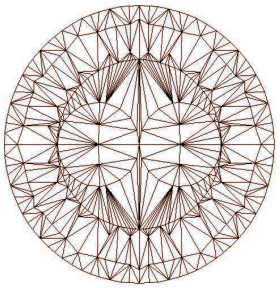

Fig. 8. Initial mesh of the two-cylinder rotor at the aligned position.

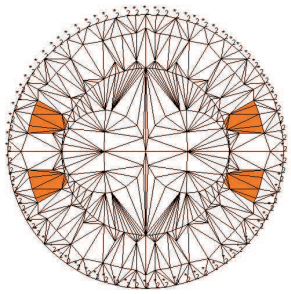

Fig. 9. Boundary conditions.

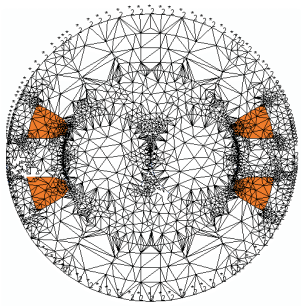

Fig. 10. The mesh after adaptation.

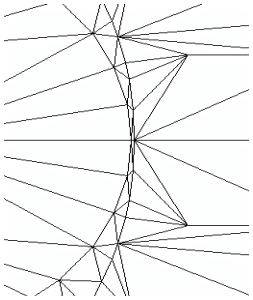

Fig. 11. Part of the air gap before adaptation.

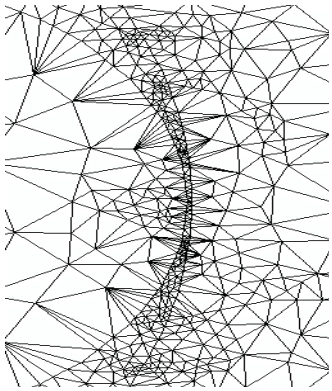

Fig. 12. Part of the air gap after adaptation.

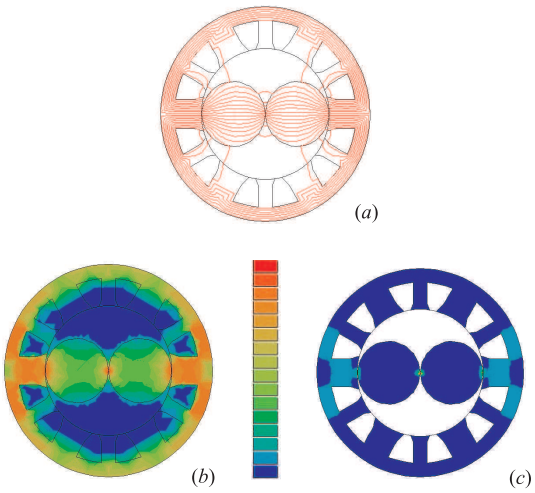

Fig. 13. The magnetic flux plot, the flux density distribution, and the saturation ratio: (a) The magnetic flux plot (aligned position); (b) the flux density distribution (aligned position); (c) the saturation ratio (aligned position).

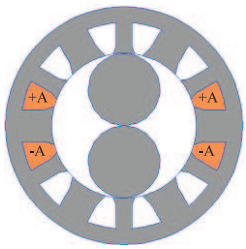

Fig. 14. One phase energized of the proposed two-cylindrical rotor SRM.

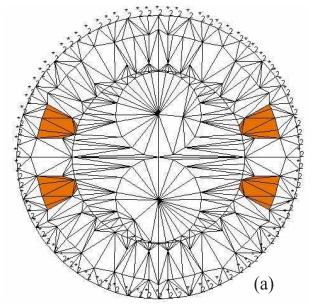

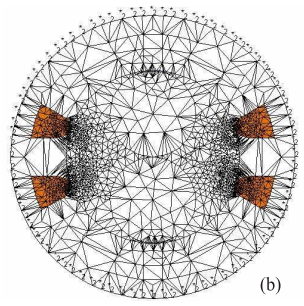

Fig. 15. Meshes before and after adaptations (unaligned position): (a) The coarse mesh before adaptation. Boundary conditions are inserted (unaligned position); (b)The coarse mesh after adaptation.

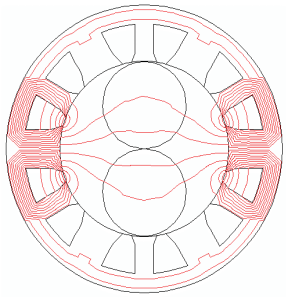

Fig. 16. The Magnetic flux plot (unaligned position).

tal connections to give as near optimal mesh as possible. At the same time, geometrical boundaries must be maintained. The automatic meshing and adaptive solution techniques are sufficiently robust and mature to allow routine employment in finite element analysis [10].

Figure 10 shows the mesh of the proposed new design after adaptation. Figure 11 shows the meshes before adaptation near the air gap and Fig. 12 shows them after adaptation.

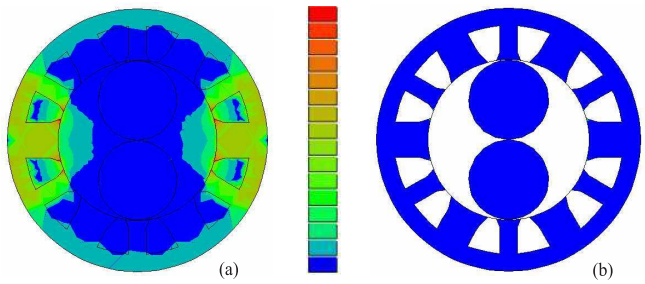

Fig. 17. Flux density and Saturation ratio (unaligned position): (a) Flux density distribution; (b) Saturation ratio.

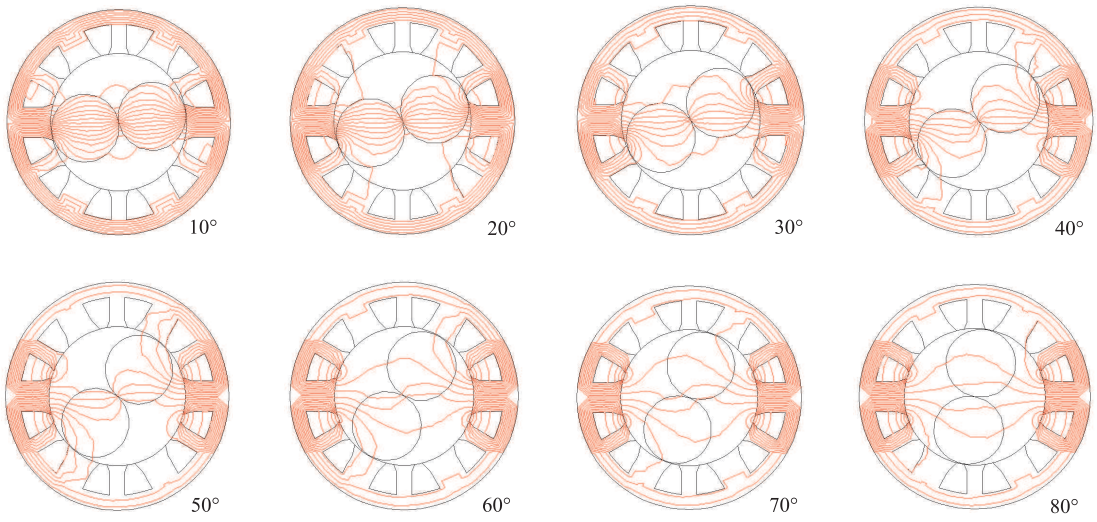

Fig. 18. The magnetic flux plot for different rotor positions - as indicated, from 10 to 80 degrees.

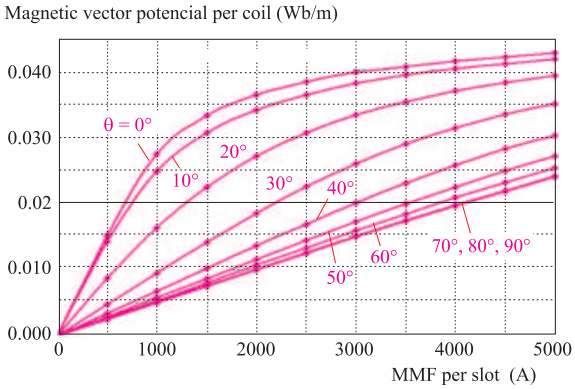

Fig. 19. The magnetic vector potential per coil (there are two coils per phase) versus the MMF per slot for the proposed machine.

There are lots of meshes near the air gap because this is the most important area in the machine as all the torque occurs in the air gap. It is clear that the meshes fit all the part and especially the small parts that cannot be modelled precisely mathematically [11].

Figure 13 (a) shows the magnetic flux plot, which indicates the percentage of the flux gone from the stator to the rotor (by counting the magnetic flux lines in the stator and the rotor).

In a proper design, most of the stator flux goes to the rotor. Figure 13 (b) shows the flux density distribution. In this figure the flux density distribution near the conductors has the highest flux density. Figure 13 (c) shows the saturation ratio (the ratio of the flux in a given part of the magnetic circuit to the flux in the tooth with the energized windings on it) in each section of the machine. There is not unwilled over-saturation in the aligned position. This means the flux is distributed uniformly, which maximizes the inductance in the aligned position.

Figure 14 shows the windings of one phase when it is in the unaligned position. Figure 15 shows meshes before and after adaptation. The figure clarify the boundary condition: the outside stator diameter is assumed to be a zero equipotential surface. The orange colour shows the location of one phase conductors.

The magnetic flux plot for the unaligned position is shown in Fig. 16. Few magnetic flux lines cross from the stator to the rotor, which proves that the new design has maximum reluctance in the unaligned position.

Figure 17 (a) shows flux density distribution in the unaligned position. The flux density is low in all parts of the machine except around the conductors where it is slightly high. This means the reluctance in the unaligned position is high. Figure 17 (b) shows the saturation ratio in the machine in the case of unaligned position.

Figure 18 shows the magnetic flux plot for different rotor positions. The magnetic flux lines increases inside the machine when the rotor moves from the unaligned position to the aligned position.

Figure 19 shows the magnetic vector potential per coil (there are two coils per phase) versus the MMF per slot.

Figure 20 shows the general shape of the flux linkage and static torque characteristics of the proposed SRM assuming there are two coils per phase each coil has 300 turns.

4 THE PERFORMANCE OF THE NEW ROLLED ROTOR SRM

The machine performance has been predicted analytically from the fundamental equation of the terminal voltage of any machine:

$$V = Ri + \frac{\partial \psi}{\partial t}$$

Then by solving one of the following first order differential equations [12–14]:

$$v = Ri + \frac{\mathrm{d}i}{\mathrm{d}t}\frac{\partial \psi}{\partial i}(\theta, i) + \omega \frac{\partial \psi}{\partial \theta}(\theta, i)\,,$$

$$v = Ri + \frac{\mathrm{d}i}{\mathrm{d}t}\frac{\partial \psi(\theta, i)}{\partial i} + \omega \frac{\partial \psi(\theta, i)}{\partial \theta}\,,$$

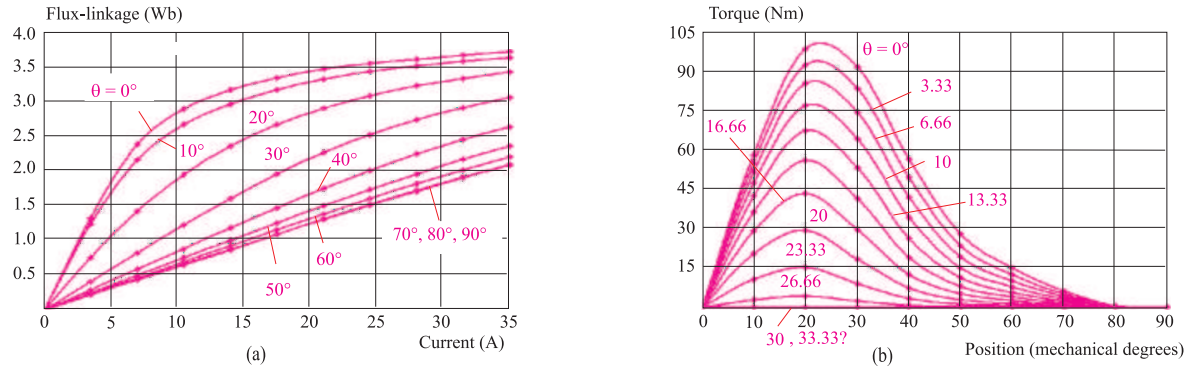

Fig. 20. The characteristics of the proposed SRM: (a) Flux linkage; (b) Torque.

$$v = Ri + \frac{\mathrm{d}i}{\mathrm{d}t}L(\theta, i) + \omega\frac{\partial L}{\partial\theta}(\theta, i)\,,$$
$$v = Ri + \frac{\mathrm{d}i}{\mathrm{d}t}L(\theta, i) + \omega\frac{\mathrm{d}L(\theta, i)}{\mathrm{d}\theta}\,.$$

numerical approach to the simulation of SRMs has been introduced in [12–13]. The flux-linkage can be determined from this equation:

$$\psi = \int \big(v - Ri(\theta, \psi)\big)\delta t\,.$$

The torque can be obtained indirectly from the co-energy:

$$W'(\theta, i) = \int_0^i \psi(\theta, i)\mathrm{d}i\Big|_{\theta=\mathrm{const}}\,,$$
$$T(\theta, i) = \frac{\mathrm{d}W'(\theta, i)}{\mathrm{d}\theta}\Big|_{i=\mathrm{const}}\,.$$

Figure 21 shows the block diagram of the SRM simulation package. The flux linkage characteristic data is taken from an adaptive finite element solution of the magnetic characteristics. It is stored in tables (one for the flux-linkage characteristic and one for the torque), then loaded in to a simulation of the SRM using Matlab/Simulink [12, 13].

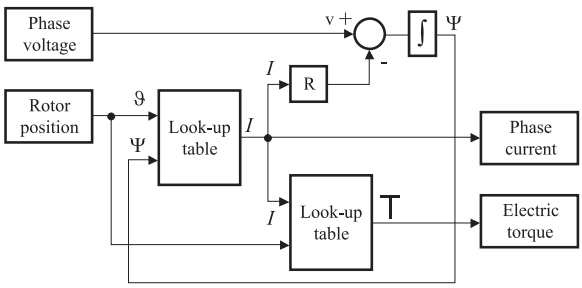

Fig. 21. Block Diagram of SRM Simulation.

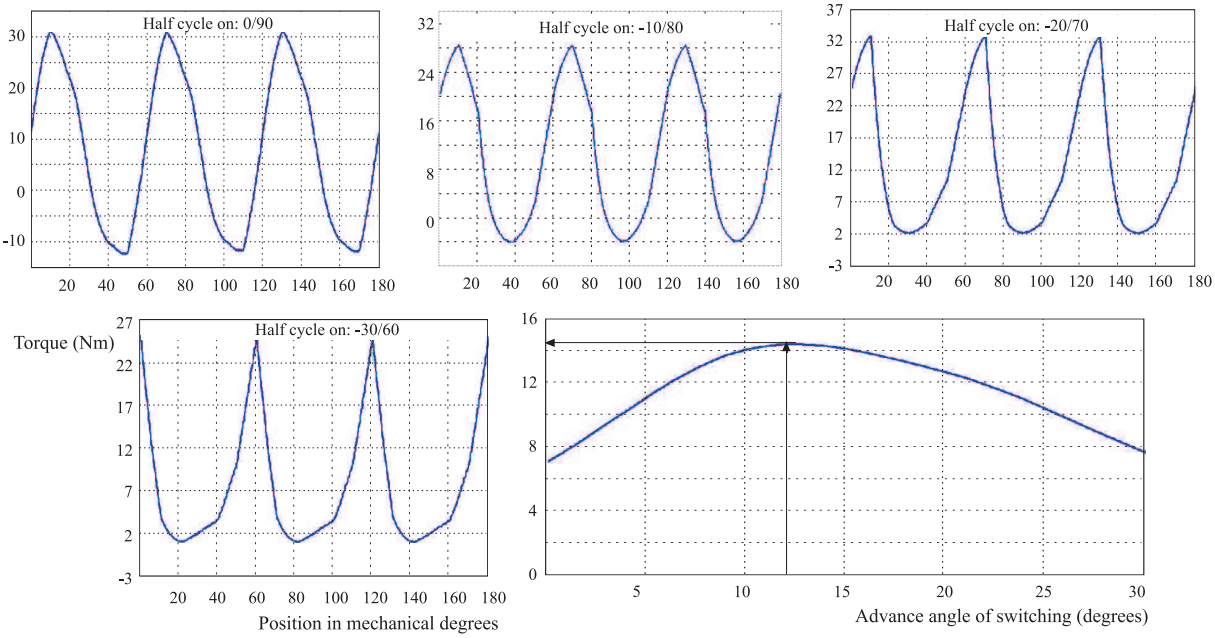

Fig. 22. Torque for different switching on angles. The motor runs under current control. The maximum value of the current is 12 A.

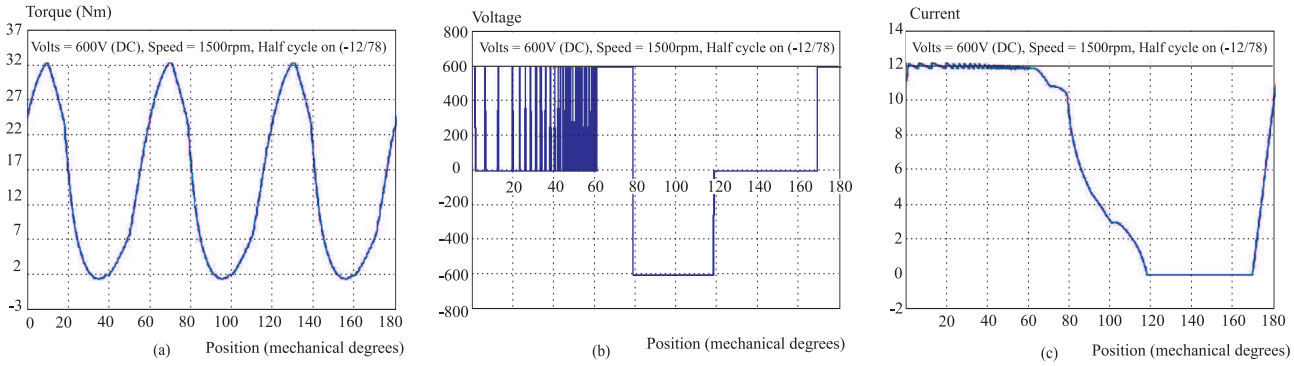

Fig. 23. The performance of the proposed SRM when the advance angle of switching on is 12 degrees.

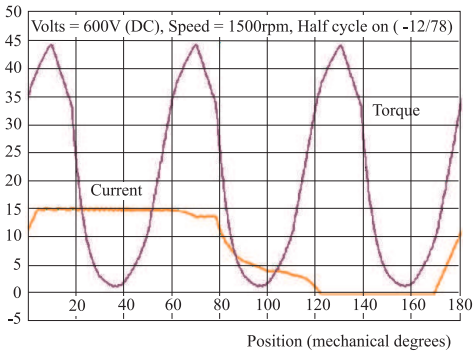

Fig. 24. Torque characteristic when the maximum value of the current is 15 A (the machine runs under current control).

As Fig. 22 shows, when all the operating conditions are kept constant the torque increases with the increase in the advance angle of switching on until certain value then the torque decreases. So, there is an optimum value of advance switching on at which the motor produces the maximum torque.

Figure 23 shows the dynamic performance of the new SRM for the operating conditions: the advance angle of switching on is 12 degrees, the DC voltage of the converters is 600 V and the running speed is 1500 rpm. As Fig. 24 shows, the torque increases when the machine runs under current control. This means when the maximum value of the current increases the torque increases.

5 CONCLUSIONS

This paper presented a new design to the SRM. In the proposed design, the rotor topology is changed. The rotor is replaced by another rotor in order to use all the volume inside the stator in producing torque. The new rotor consists of two iron cylinders. The two cylinders are used as rotor and no need for a shaft. In addition, using this new rotor smoothes the reluctance variation consequently decreasing the torque ripples. The paper uses the adaptive finite element to model the new SRM and to predict its characteristic. MATLAB was used to perform simulations to study the performance of the new SRM. Additionally, the paper presented simulation results of the dynamic performance of the proposed SRM.

References

[1] SANADA, M.—MORIMOTO, S.—TAKEDA, Y.—MATSUI, N.: Novel Rotor Pole Design of Switched Reluctance Motors to Reduce the Acoustic Noise, IEEE Conf. IA 2000, Italy.

[2] XU, L.—TANG, Y.—YE, L.: Comparison Study of Rotor Structures of Doubly Excited Brushless Reluctance Machine by Finite Element Analysis, IEEE Transactions on Energy Conversion **9** No. 1 (March 1994).

[3] LI *et al*: Axial Flux Reluctance Machine with Two Stators Driving A Rotor, US Patent, US 5925965, Jul. 20, 1999.

[4] RAO: Ac Synchronous Motor Having an Axially Laminated Rotor, US patent, US 4110646, 29/8/1978.

[5] FISHER, E. A.—RICHTER, E.: Conical Rotor for Switched Reluctance Motor, US5233254, US-Patent, 3/8/1993.

[6] KLIMAN: Composite Rotor Lamination For Use in Reluctance Hompolar, and Permanent Magnet Machines, US patent, US4916346, 10/4/1990.

[7] NAOYUKI, S.—YUKIO, H.—HIROSHI, M.—SHIZUKA, Y.: Rotor for Reluctance Motor, Japanese Patent, no. 10150753 (2/6/98).

[8] NEILSON, F. N.: Operation of Switched Reluctance Machines' European Patent, EP 0959555, 24/11/1999.

[9] MURTHY, S. S.—SINGH, B.—SHARME, V. K.: Finite Element Analysis to Achieve Optimum Geometry of Switched Reluctance Motor, IEEE IAS (1998), 414–418.

[10] JACK, A. G.—FINCH, J. W.—WRIGHT, J. P.: Adaptive Mesh Generation Applied to Switched-Reluctance Motor Design, IEEE Transaction On Industry Applications **28** No. 2 (March/April 1992).

[11] JACK, A. G.: Automation of the Design Process for Electrical Machines, International Conference on Electrical Machines and Power Electronics' Kusadasi-Turkey 27–29 May 1992, CEMP 92.

[12] CHANDRASEKHARA, E. S. paper Dynamic Performance of Reluctance Motors with Magnetically Anisotropic Rotors: IEEE Transactions on Power Apparatus and Systems **. PAS-95** No. No 4 (July/August 1976).

[13] XU, L.—RUCKSTADTER, E.: Direct Modelling of Switched Reluctance Machine by Coupled Field-Circuit Method, IEEE Transactions on Energy Conversion **10** No. 3 (September 1995).

Received 3 February 2006

Eyhab El-kharashi (Dr) received his PhD degree in the electrical machines design from University of Newcastle upon Tyne, UK in 2003 and BSc (first class honours) and MSc degrees in electrical Power and Machines Engineering from Ain Shams University, Cairo, Egypt, in 1994 and 1997 respectively. Now he is an assistant professor in the Department of Electrical Power and Machines, Faculty of Engineering, Ain Shams University, Cairo, Egypt. His research interests include electrical machines design.